The effects of actomyosin disruptors on the mechanical integrity of the avian crystalline lens

Gah-Jone Won,[1] Douglas S. Fudge,[2] Vivian Choh[1]

[1]*School of Optometry and Vision Science, University of Waterloo, Ontario, Canada;* [2]*Department of Integrative Biology, University of Guelph, Guelph, Canada*

Purpose: Actin and myosin within the crystalline lens maintain the structural integrity of lens fiber cells and form a hexagonal lattice cradling the posterior surface of the lens. The actomyosin network was pharmacologically disrupted to examine the effects on lenticular biomechanics and optical quality.

Methods: One lens of 7-day-old White Leghorn chickens was treated with 10 µM of a disruptor and the other with 0.01% dimethyl sulfoxide (vehicle). Actin, myosin, and myosin light chain kinase (MLCK) disruptors were used. The stiffness and the optical quality of the control and treated lenses were measured. Western blotting and confocal imaging were used to confirm that treatment led to a disruption of the actomyosin network. The times for the lenses to recover stiffness to match the control values were also measured.

Results: Disruptor-treated lenses were significantly less stiff than their controls ($p \leq 0.0274$ for all disruptors). The disruptors led to changes in the relative protein amounts as well as the distributions of proteins within the lattice. However, the disruptors did not affect the clarity of the lenses ($p \geq 0.4696$ for all disruptors), nor did they affect spherical aberration ($p \geq 0.2245$). The effects of all three disruptors were reversible, with lenses recovering from treatment with actin, myosin, and MLCK disruptors after 4 h, 1 h, and 8 min, respectively.

Conclusions: Cytoskeletal protein disruptors led to a decreased stiffness of the lens, and the effects were reversible. Optical quality was mostly unaffected, but the long-term consequences remain unclear. Our results raise the possibility that the mechanical properties of the avian lens may be actively regulated in vivo via adjustments to the actomyosin lattice.

The process of accommodation allows for the eye to focus on nearby objects. The mechanism by which this occurs in vertebrates involves either a translation of the lens or a change in the lens curvature to increase the optical power of the eye [1]. Humans and birds are similar in that both species use the latter method to accommodate [1,2]. However, the changes in the human lens occur via the relaxation of zonules attached to the ciliary muscle [1,3], whereas the ciliary muscle in the avian eye directly articulates with the equator of the lens [2], resulting in a squeezing of the lens in the equatorial plane.

The lens maintains its integrity and transparency due to the organization of its cells, which are epithelial in origin [4-6]. Similar to other epithelial cells in the body, lens epithelial cells contain cytoskeletal filaments, the smallest of which are known as microfilaments and are found throughout the lens [7]. Microfilaments are composed largely of filamentous f-actin and are responsible for an array of essential biologic functions, including facilitating changes in cell shape, fortifying cell–cell and cell–extracellular matrix interactions, and compartmentalizing plasma membranes [8,9].

In most cells, the f-actin function relies on its ability to interact with myosin II, a non-muscle and smooth muscle motor protein, to form actomyosin assemblies [10]. In smooth- and non-muscle systems, the contraction of actin and myosin is triggered by myosin light chain kinase (MLCK), an upregulator of ATPase activity and a catalyst for actin-myosin cross-linking [11-13]. The ATP is used by myosin heads to move along actin filaments and results in the contractile movement of myofilaments. In squirrels, rabbits, and humans, f-actin is arranged in polygonal arrays at the anterior faces of crystalline lenses and is associated with myosin within the epithelium [14]. Similarly, at the posterior surface of the avian crystalline lens, f-actin, non-muscle myosin, and N-cadherin are arranged in a hexagonal lattice resembling a "two-dimensional muscle" [15]. The actomyosin complex at the anterior epithelium has been speculated to facilitate accommodation by allowing the epithelial cells to change shape or by permitting the lens as a whole to change into a more spherical shape [16]. Furthermore, the proteins collectively at the basal membrane complex (BMC) of the posterior lens surface have been shown to mediate fiber cell migration across, and anchor fiber cells to, the lens capsule [15]. In addition, the presence of highly regular actomyosin lattices in the lens raises the possibility that these networks are involved in setting the passive biomechanical response

Correspondence to: Vivian Choh, 200 University Ave West, Waterloo, ON, N2L 3G1 Canada, Phone: +1 519 888-4567 x35005; FAX: +1 519 725-0784; email: vchoh@uwaterloo.ca

of the avian lens to external forces, such as those exerted by the ciliary muscle. Indeed, previous research using knockout mice has shown that in the murine lens, beaded filaments, which are intermediate filaments unique to the lens, contribute significantly to lens stiffness [17]. Furthermore, the fact that the actomyosin network has the potential to be contractile raises two even more intriguing possibilities: that lens stiffness could be actively tuned by adjusting the amount of tension in the network and that the shape of the lens itself could be similarly adjusted [15,16,18-20]. The demonstration that the MLCK inhibitor, ML-7, has significant effects on the focal length, and therefore almost certainly the shape of avian lenses seems to support this idea [21]. The purpose of this study was to test the hypothesis that lenticular actomyosin networks affect the biomechanics and optics of the whole avian lens by pharmacologically disrupting them and measuring the effects on lens stiffness and optical clarity.

METHODS

Animals: White leghorn (*Gallus gallus domesticus*) hatchling chicks were obtained from the Maple Leaf hatchery in New Hamburg, Ontario and were fed ad libitum. They were housed in stainless steel brooders with a heat source and kept on a 14 h:10 h light-dark cycle. Chicks were raised in accordance with the Guidelines of the Canadian Council on Animal Care and with the ARVO Statement for the Use of Animals in Ophthalmic and Vision Research. As the focus of this study was to test the fundamental question of whether disrupting cytoskeletal proteins could have an effect on lenticular biomechanics, chicks with robust amounts of accommodation (about a week old) were used instead of older birds, which will be considered for a future study once the functions of disruptors have been well established. Week-old chicks also show highly monotonic spherical aberrations (SAs) [22], thereby providing a model against which optical changes could be assessed.

Lens dissections: Chicks that were 6–8 days old were sacrificed by decapitation and their eyes were enucleated. Eyes were placed in chilled oxygenated Tyrode's solution (TS: 134 mM NaCl, 3 mM KCl, 20.5 mM NaHCO$_3$, 1 mM MgCl$_2$, 3 mM CaCl$_2$) before removal of the posterior globe and vitreous humor. The exposed lens was then separated from the surrounding ciliary body and extracted from the anterior segment, taking care to minimize damage to the lens capsule.

Disruptors: Latrunculin A (LAT-A) is a drug that rapidly, reversibly, and specifically disrupts actin cytoskeleton by preventing polymerization [23,24]. As well, 1-phenyl-1,2,3,4-tetrahydro-4-hydroxypyrrolo[2.3-b]-7-methylquinolin-4-one (blebbistatin) is a reversible inhibitor with a specificity

and high affinity for several class II myosins and acts by reducing the actin affinity of the myosin heads [25]. Finally, 1-(5-Iodonaphthalene-1-sulfonyl)-1H-hexahydro-1,4-diazepine hydrochloride (ML-7) selectively disrupts MLCK activity by preventing myosin II light-chain phosphorylation [26].

Lens treatments: For each bird, one eye was treated for 15 min with either 10 µM latrunculin (n = 18) in 0.01% (v/v) dimethyl sulfoxide (DMSO) in TS, 10 µM blebbistatin (n = 16) in 0.01% (v/v) DMSO in TS, or 10 µM ML-7 (n = 14) in 0.01% (v/v) DMSO in TS. The lenses from the opposite eyes were subjected to a vehicle (0.01% (v/v) DMSO in TS; 15 min). Assignment to the treatment group alternated between left and right eyes. All lenses were briefly rinsed in TS before biomechanical testing, western blot analysis, immunocytochemical processing, or assessment of optical quality.

Lens compressions: The mechanical properties of the lenses were measured using a universal testing machine (Instron, Norwood, MA). Each lens was placed anterior side down on a pedestal located in the compression chamber containing chilled TS (Figure 1). Lenses were then compressed by 0.75 mm using an aluminum compression element connected to a 10-N load cell, and measurements of the resultant force exerted by the lenses were collected. For experiments examining whether the effects on the biomechanics were reversible, a 5-N sensitive load cell was used and compressions were performed in disruptor- and vehicle-free TS. This was done immediately after the 15 min disruptor/vehicle treatment at the following time points: 1 min, 2 min, 4 min, 8 min, 16 min, 32 min, 1 h, 2 h, 4 h, 8 h, 16 h, and 32 h after treatment. The force compression data for each lens were collected using Bluehill software (ver. 9, Instron).

Analysis of stiffness: Force data were adjusted to account for the buoyancy exerted by the surrounding solution on the compression element, as it displaced more or less test solution during compression and relaxation of the lens. The resulting
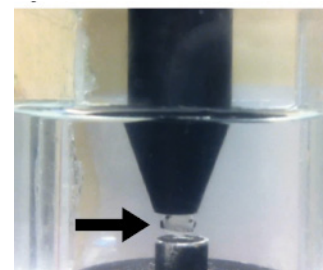

Figure 1. Image of a lens in the compression chamber. The lens (arrow) is submerged in TS, sitting anterior side up on a pedestal and compressed from above by an aluminum compression element connected to a load cell.

force-compression curves that were generated for each lens were then best fit to a three-parameter exponential curve with the equation $y = y_0 + ae^{bx}$. As the b-coefficient of the exponential equation is a unitless constant that describes the relationship of how rapidly the force increases as the compression distance increases, it was used to assess the relative stiffness between lenses [27,28] with larger numerical values for the b-coefficient representing steeper curves, and thus stiffer lenses. B-coefficients from each curve were extracted, and means and standard deviations were calculated from these data. Dimensionless b-coefficient values for whole lenses should not be confused with the Young's Modulus, which is known to vary in different parts of the lens [29] and was not measured in this study. It should be noted there were no significant differences in the sizes of the control and treated lenses; thus, differences in the b-coefficients likely correspond to differences in the Young's Modulus of at least part of the lens, although our data cannot tell us which part.

Western blot: A western blot analysis was performed to confirm that disruptors had the expected effects on the lenses. Disruptor and vehicle treatments were identical to those for the compression trials. Lenses were dissected and separated into 1) BMC samples, which include posterior capsule and sheared ends of lens fiber cells still attached to the membrane, and 2) decapsulated lens fiber samples, composed of cortical and nuclear fibers. Each sample was separately ground using mini pestles and lysed with radioimmunoprecipitation assay buffer (RIPA; R0278, Sigma-Aldrich Co., Oakville, ON, Canada) containing a general use protease inhibitor cocktail (P2714, Sigma-Aldrich Co.). The total protein of the lens tissue samples was quantified using the BioRad DC protein assay (500−0111; BioRad Laboratories, Inc., Mississauga, ON, Canada). Samples were prepared with a Laemmli sample buffer, run on 10% precast gels (456−1033, BioRad Laboratories, Inc.) in the BioRad Mini-Protean System (165−8000, BioRad Laboratories, Inc.), transferred to a polyvinyldene fluoride (PVDF; 162−0175, BioRad Laboratories, Inc.) membrane, and visualized with antibodies specific to the protein being blotted. Mono- and polymeric actin levels in the lens capsule were quantified using a globular (g-) actin/filamentous (f-) actin in vivo assay biochemistry kit (BKO37, Cytoskeleton, Inc., Denver, CO). In brief, lens samples were homogenized, and a detergent-based lysis buffer that stabilizes and maintains the globular and filamentous forms of cellular actin was added. The lysate containing each sample was then centrifuged (21,100 × *g*, Thermo Scientific Sorvall Legend Micro) [21], with the resulting supernatant and pellet containing g-actin and f-actin, respectively. Actin levels in both the supernatant and pellet were then quantified by a western blot analysis for three replicates, each consisting

of a minimum of four lens tissue extracts. ML-7 inhibits MLCK, which phosphorylates myosin; therefore, antibodies against phosphorylated myosin (M6068, Sigma-Aldrich) were used for ML-7-treated samples. An anti-beta actin antibody (ab8224, Abcam Inc., Toronto, ON, Canada) was used as a loading control. Secondary antibodies conjugated with horseradish peroxidase were detected by enhanced chemiluminescence using Amersham ECL prime (RPN2236, GE Healthcare, Mississauga, ON, Canada). Western blots were visualized using a Storm 860 scanner (GE Healthcare) and assessed using the ImageQuant software (GE Healthcare).

Optical quality: The optical quality of the lenses was assessed using a ScanTox© scanning laser monitor. In brief, lenses were placed anterior side down in a rectangular glass chamber in TS and 5% fetal bovine serum, with the latter used to visualize the helium-neon laser beams passing through the lens at various eccentricities from the optical axis. Refracted beams were captured and recorded with a camera, and back vertex focal lengths were calculated using software associated with the scanner. Beams passing through the sutures were omitted, as they produce highly inaccurate back vertex focal lengths. The optical quality of the lenses was assessed based on changes in scatter and spherical aberration (SA). For calculations of SA, data were first converted to dioptric values (vergences) using a thin lens approximation in water; the refractive index of water ($n_w = 1.33$) was divided by the back vertex focal lengths (in meters). The vergences were then fitted using a third-order polynomial line of regression to determine the back vertex distance at the optical axis (Figure 2). The amounts of SA were determined for a 1.5 mm pupil size by averaging the SA calculations for the positive (0 to 0.75 mm) and negative (0 to −0.75 mm) eccentricities. As bird lenses typically show a high negative SA [22,30-32], scatter was quantified as the mean deviation of the various focal lengths from the best fitting third-order polynomial line of regression. Higher deviations indicated higher degrees of scatter.

Confocal microscopy: Blebbistatin- and latrunculin-treated lenses and the controls for these lenses were fixed with 2% (v/v) paraformaldehyde in TS. Lenses were permeabilized in toto using 0.05% v/v Triton X-100 in PBS before the addition of a mouse anti-myosin-light-chain antibody (M4401, Sigma-Aldrich, 1:100 dilution in PBS, 2 h at 37 °C) followed by a rabbit anti-mouse secondary antibody conjugated to Texas Red (1:500 in PBS, overnight at RT). Following a 3×5 min wash, lenses were counterstained with phalloidin FITC (P5282, Sigma-Aldrich, 1:400 dilution in PBS, 15 min, RT). Lenses were mounted in toto posterior pole up onto slides using 5% (w/v) agar solution in water with 0.05 mg/
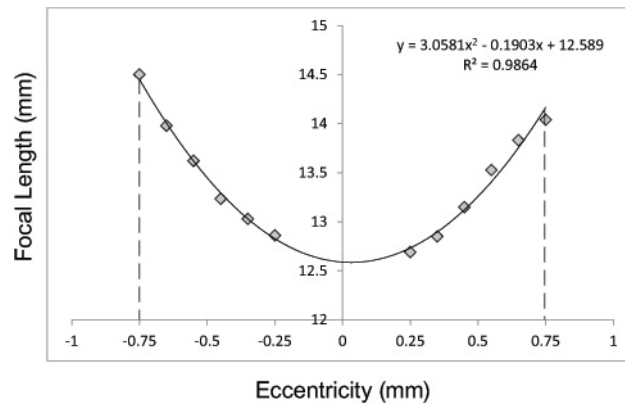
Figure 2. Effects of disruptors on lenticular optics. Line graph showing the focal length (mm) at various eccentricities (mm) of a typical avian crystalline lens. Graphs were fitted with third-order polynomial equations to calculate the amount of scatter and SA.

ml phenylenediamene (P6001, Sigma-Aldrich; in 50% (v/v) glycerol in water). A coverslip coated with ProLong Gold (P36934, Life Technologies) was then placed on top of the posterior pole of the lens and adhered to the slide with the agar. The protein distribution of lenses was visualized using a Zeiss LSM 510 confocal microscope and images were captured and processed using the Zen 2011 software (Zeiss).

Nearest neighbor analysis: Protein distributions were quantified using a nearest neighbor analysis, which assesses the closeness of points of interest (POIs) on an image and assigns a value between 0 and 2.15, where a score of 0 represents clustered POIs, a score of 1 represents a random distribution of POIs, and a score of 2.15 is a highly regular distribution of POIs. For latrunculin-treated lenses (n = 3), the POIs used were the vertices of actin hexagons, while for blebbistatin-treated lenses (n = 3), the POIs used were the center of myosin globules. POIs were targeted and selected using NIH Image or Scion Image software. Nearest neighbor values (R_n) were calculated using the equation

$$R_n = D(Obs) / 0.5\sqrt{\frac{a}{n'}}$$

Where DObs) is the mean observed nearest neighbor distance, a is the area, and n is the total number of POIs.

Statistical analysis: The effects of the disruptors on the stiffness and optical quality of the lenses were analyzed using a mixed-model analysis of variance (ANOVA), with disruptor versus vehicle as the repeated measure and the type of disruptor used as a factor. For the longitudinal (reversibility) study, a two-way repeated-measured ANOVA was used with the disruptor versus vehicle as one measure and time as the other. Tukey or Bonferroni-corrected post-hoc multiple comparison tests were performed where applicable. Comparisons of the optical quality of the lenses, as well as of nearest neighbor values were assessed using paired *t* tests.

For all statistical tests, results were considered significant at p≤0.05.

RESULTS

Force-compression curves were generated for each lens (Figure 3). A linear regression of the data to a three-parameter exponential curve (y = y + ae^{bx}) yielded mean r^2 values (± SEM) of 0.9861±0.0217 (range: 0.8787 and 0.9999). For most pairs of lenses, treatment with disruptors was associated with a decrease in the stiffness of the lens, as indicated by the shallower force-compression curves (Figure 3, solid grey lines and filled symbols). Specifically, for 15 of 18 pairs of eyes in the latrunculin group, treated lenses exhibited relatively lower stiffness values for the latrunculin-treated lenses compared to the vehicle-control, while three pairs showed the opposite trend, with stiffness in the latrunculin-treated lenses being relatively higher than in those exposed to the vehicle. The mean stiffness values reflected the general trend, with latrunculin-treated lenses being significantly lower (± SEM) at 2.64±1.28 compared to the vehicle-treated lenses at 4.15±1.15 (p = 0.0011; Figure 4A). Similarly, 14 of 16 pairs of lenses showed relatively lower stiffness values for the blebbistatin-treated lenses compared to the vehicle-treated counterparts, with two pairs showing the opposite trend. Again, the mean stiffness values (± SEM) were lower for the blebbistatin-treated lenses (3.25±0.23) than for those exposed to the vehicle (4.47±0.57; p = 0.0274; Figure 4B). Finally, for 12 of 14 pairs of lenses, the stiffness values of the ML-7 treated lenses were relatively lower compared to the vehicle-treated lenses, while the values for two pairs of lenses were relatively higher. The mean stiffness value for the ML-7-treated lenses was, again, lower than for the counterpart eyes (2.90±1.19 versus 4.49±1.23, respectively; p = 0.0027; Figure 4C). A mixed model analysis revealed neither significant differences in the stiffness levels between the disruptors (p = 0.2379) nor an interaction effect (p = 0.7483).

A western blot analysis indicated that latrunculin and ML-7 treatments were effective in disrupting actin levels and myosin phosphorylation, respectively, at both the BMC and the lens fibers. Actin levels in latrunculin-treated lenses were quantified using a g-actin/f-actin in vivo assay kit, which revealed a large decrease in f-actin both at the BMC and in the lens fiber cells as a result of lens tissue treatment. In BMC samples treated with latrunculin, the mean intensity (± SEM) of f-actin was 12.0±1.2, while the mean intensity of g-actin was 19.3±1.9, representing 38.4±0.5% and 61.6±0.5% of the total actin amount, respectively, indicating substantial depolymerization of f-actin as a result of latrunculin treatment (Figure 5A, top panel). In comparison, control samples showed a ratio of approximately 1:1, with mean intensities of f- and g-actin at 14.2±1.4 and 13.7±1.4, representing 51.0±0.5% and 49.0±0.5% of the total actin amount, respectively. In the lens fiber samples treated with latrunculin, the mean intensity (± SEM) of f-actin was 10.0±1.6, while the mean intensity of g-actin was 18.3±1.9, representing 35.4±0.6% and 64.7±0.7% of the total actin amount, respectively (Figure 5A; bottom panel). In comparison, control samples again showed a ratio of approximately 1:1, with mean intensities of f- and g-actin at 13.4±1.3 and 13.3±1.2, representing 50.1±0.5% and 49.9±0.5% of the total actin amount, respectively. The relative intensities of phospho-myosin were lower in both BMC (by 49.8%; treated versus control: 18.6±3.0 versus 55.5±1.9, respectively) and lens fiber cell samples (by 35.7%; treated versus control: 9.1±2.2 versus 19.2±3.1, respectively) when treated with ML-7 (Figures 5B, left and right panels, respectively), indicating an ML-7-dependent inhibition of myosin phosphorylation.

Confocal images indicated that latrunculin led to the rearrangement and thinning of the actin cables at the basal membrane (Figure 6). Actin in the latrunculin-treated lenses appeared different from the vehicle-treated lenses, which showed the typical punctate staining of the highly regular hexagonal vertices. Additionally, myosin bundles localized at the center of the actin formations appeared more variable in size and neighboring distance. A nearest neighbor analysis indicated a significant increase in the disorder of the myosin associated with the actin lattice (R_{nm} for treated lenses:
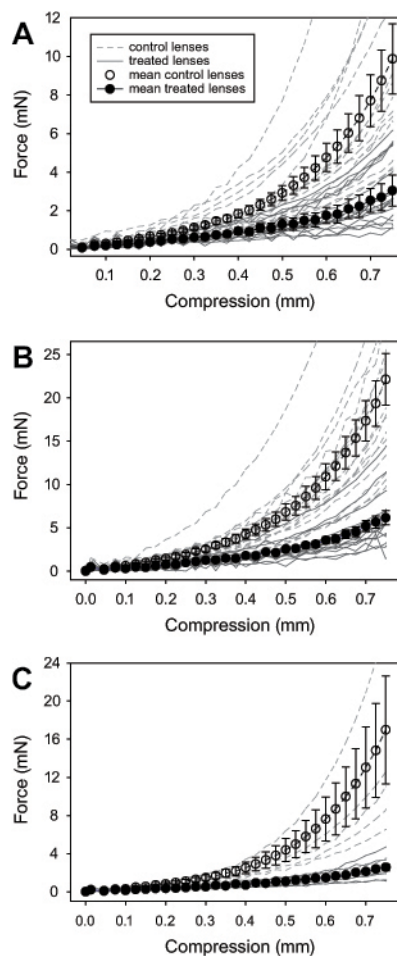

Figure 3. Force-compression curves of all lenses. Mean force ± SEM of (**A**) latrunculin-, (**B**) blebbistatin-, and (**C**) ML-7-treated lenses (filled symbols) and their controls (empty symbols), as a function of compression. Force-compression curves of individual disruptor-treated (solid gray lines) and vehicle-treated (dashed gray lines) lenses are also included.
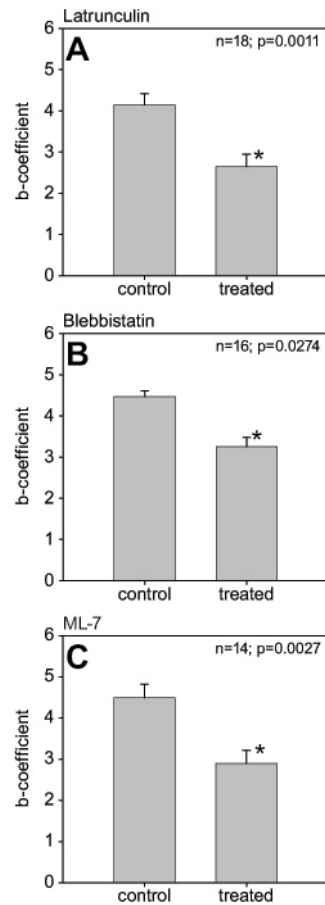
Figure 4. Effects of disruptors on lenticular stiffness. Mean stiffness values ± SEM of disruptor- and vehicle-treated lenses for (**A**) 10 μM latrunculin (n = 18), (**B**) 10 μM blebbistatin (n = 16), and (**C**) 10 μM ML-7 (n = 14). Asterisks denote significant differences (all groups p≤0.0274).
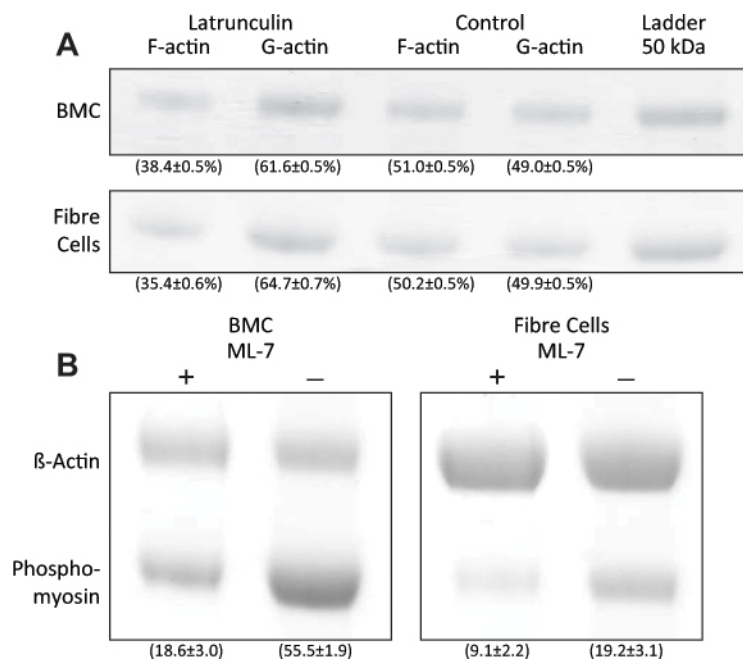

Figure 5. Effects of disruptors on protein concentrations in the lens. (**A**) Western blots of f- and g-actin in BMC and lens fiber cell samples treated with latrunculin. Numbers in parentheses represent the mean percentage optical density (±SEM) relative to the total amount of actin. (**B**) Western blots of phospho-myosin in BMC and lens fiber cell samples treated with ML-7. Numbers in parentheses represent the mean optical densities (±SEM). β-actin was used as the loading control.
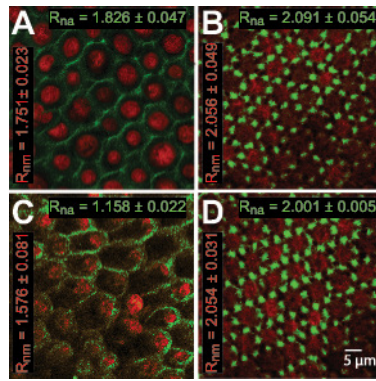
Figure 6. Effects of disruptors on actin and myosin distributions in the lens. Confocal images of posterior lens capsules showing the distribution of actin (green) and myosin (red) in a (**A**) latrunculin-treated lens and (**B**) its vehicle-treated counterpart, as well as a (**C**) blebbistatin-treated lens and (**D**) its vehicle-treated counterpart. Scale bar = 5 µm for all images. R_n values for actin (R_{na}, green) and myosin (R_{nm}, red) distributions are included.

1.751±0.023 versus R_{nm} for control lenses: 2.056±0.054; p = 0.0025). The actin distribution in latrunculin-treated lenses had an R_{na} (± SEM) of 1.826±0.047, while its vehicle-treated counterpart had an R_{na} of 2.091±0.054, indicating a small increase in f-actin disorder (Figures 6A, B), although these changes were not significant (p = 0.0593).

Both actin and myosin organizations were adversely affected by blebbistatin. The myosin distributions in lenses treated with blebbistatin were even less ordered than those observed in latrunculin-treated lenses, and treated lenses showed an even lower R_{nm} of 1.576±0.081, while their vehicle-treated counterparts had an R_{nm} of 2.054±0.031 (p = 0.0183, Figures 6C, D). The actin distribution was also affected; blebbistatin-treated lenses lost the regular repeating arrays of punctate staining, and the R_{na} of 1.158±0.022 in these lenses was significantly different from that in the control lenses, at an R_{na} of 2.001±0.005 (p = 0.0183), indicating a large increase in disorder.

Despite the rearrangement of the cytoskeletal proteins at the BMC, the optical quality of disruptor-treated lenses, assessed using two criteria, scatter and SA (Table 1), were unaffected. The disruptor-treated lenses showed neither a difference in the amounts of scatter compared to their respective controls (p≥0.4696; Table 1) nor did any disruptor treatments result in differences in the amount of SA (p≥0.2245; Table 1). In the longitudinal (reversibility) compression trials, it was found that lenses treated with latrunculin took the longest to recover, showing significant differences in stiffness up until the 4-h mark, (mean stiffness ± SEM at 4 h: control lenses, 6.17±0.43 versus treated lenses, 4.98±0.56; p = 0.0730; Figure 7A). Lenses treated with blebbistatin were found to have a recovery time of 1 h (mean stiffness at 1 h: control lenses, 5.37±0.19 versus treated lenses, 5.27±0.51; p = 1.000; Figure 7B). Lenses treated with ML-7 had the quickest recovery time at 8 min (mean stiffness at 8 min: control lenses, 6.02±0.36 versus treated lenses, 5.17±0.40; p = 1.000; Figure 7C).

TABLE 1. MEAN SPHERICAL ABERRATION (D) ± SEM AND MEAN SCATTER (MM) ± SEM FOR LATRUN- CULIN-, BLEBBISTATIN-, AND ML-7-TREATED LENSES AND THEIR CONTROLS.

Disruptor	Spherical aberration (D)			Scatter (Mean deviation; mm)		
	Treated	Control	P value	Treated	Control	P value
Latrunculin	−11.80±0.50 (−9.13 to −13.94)	−11.57±0.48 (−9.51 to −14.30)	0.6093	1.15±0.03 (1.00 to 1.36)	1.15±0.04 (0.93 to 1.36)	0.9858
Blebbistatin	−11.62±0.31 (−9.84 to −13.13)	−11.59±0.26 (−10.13 to −12.95)	0.9212	1.19±0.07 (1.01 to 1.83)	1.14±0.02 (1.06 to 1.21)	0.4696
ML-7	−11.94±0.69 (−7.95 to −15.06)	−12.44±0.78 (−7.54 to −16.84)	0.2245	1.15±0.03 (0.91 to 1.25)	1.13±0.05 (0.81 to 1.32)	0.7526

Ranges are in parentheses.

DISCUSSION

The compression trials showed that treatment with actomyosin disruptors results in significant changes in the distributions of actin and myosin and significant decreases in the stiffness of the whole lens. While it is possible that other mechanisms were responsible for lens softening, the simplest explanation is that the decrease in stiffness was a direct result of the changes to the structure of the actomyosin lattice wrought by the disruptors. It should be noted that a small number of lenses treated with inhibitors in the compression trials showed an increase in stiffness; however, this result is likely due to the biologic variation among lenses. It is known that variations exist in lenses; lenses of the same age will show variations in thickness and the anterior surface shows a higher variation in curvature than the posterior surface. Compression forces are presumably related to the thickness and the shape of the lens; therefore, variations in both these parameters could confer variations in the compression response [33].

Responses were reversible for all three disruptors, but the kinetics of recovery differed. Latrunculin-treated lenses recovered the slowest, perhaps due to the ubiquitous presence of actin microfilaments, found not only at the lens capsule and BMC, but also within the lens cortex and nucleus, the latter two of which form the bulk of the lens [7]. More actin would presumably require more time to reassemble. Although optimal assembly conditions for actin and myosin differ, it should be noted that, at least theoretically, actin has a slower association rate than myosin II. The elongation rates of actin filaments are $11.6\pm1.2\times10^{-6}$ $M^{-1}s^{-1}$ at the barbed ends and $1.3\pm0.2\times10^{-6}$ $M^{-1}s^{-1}$ at the pointed ends [34] compared to myosin II, which has an immensely faster rate of $\geq2.0\times10^{8}$ $M^{-1}s^{-1}$ [35]. It is most likely that blebbistatin and ML-7-treated lenses were much faster in their recovery times because these disruptors do not physically segregate the target protein into its monomeric components. Instead, the myosin disruptors act by preventing phosphorylation and competitively binding to key structures in the actomyosin cascade, a process that is presumably easier and quicker to reverse [25,36].
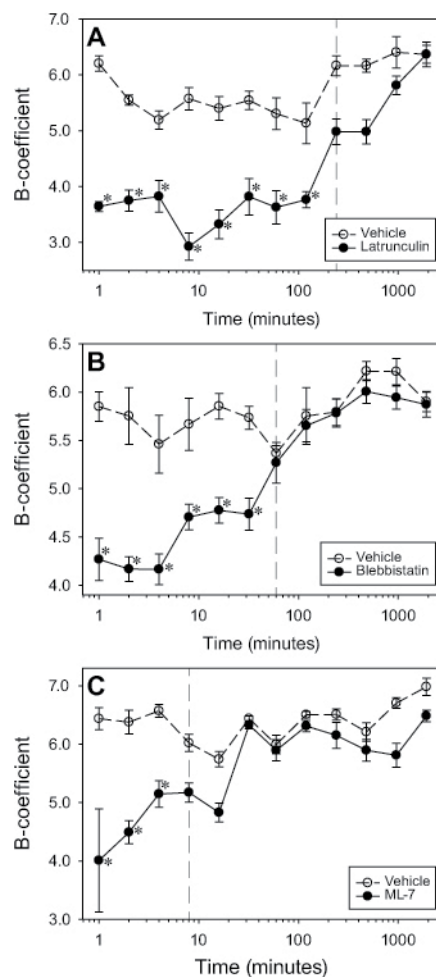

Figure 7. Time course of lenticular stiffness following disruptor removal. Longitudinal recovery effects of (**A**) 10 μM latrunculin (n = 6), (**B**) 10 μM blebbistatin (n = 6), and (**C**) 10 μM ML-7 (n = 6) on lens stiffness compared to vehicle controls. Asterisks (*) indicate significant differences between disruptor- and vehicle-treated lenses.

It should be noted that in preliminary trials, the acute treatment of lenses with a higher concentration of ML-7 (100 µM) resulted in lens stiffening, with 4 of 16 lenses physically bursting during force-compression trials (data not shown). Stiffening as a result of high concentrations of ML-7 could be due to a biphasic dose response of the MLCK inhibitor. Indeed, in the case of cell spreading, another process mediated by the dynamics of the actomyosin network, ML-7 has opposite effects in COS7 carcinoma cells when its dose is increased by a factor of five [37]. Moreover, results of two-dimensional gel electrophoresis of 100 µM ML-7-treated posterior lens capsule tissues suggest increases in protein phosphorylation compared to samples treated with 10 µM ML-7 (data not shown).

In a related study on lens shape changes by Luck and Choh [21], low and high concentrations of ML-7 resulted in longer and shorter avian lens focal lengths, respectively. Although the directionality of 10 and 100 µM changes is in agreement with the stiffening observed in our experiment, we did not observe any focal length changes with these two ML-7 concentrations. One difference may be that Luck and Choh conducted the optical trials on lenses in situ, where the lens was still in its accommodative apparatus, while we conducted our optical trials on lenses in vitro, i.e., on lenses that had been extracted from their surrounding tissue. In our experiments, lenses may have been "rounded up," a phenomenon that has been described before for lenses separated from their surrounding anatomy [38]. This idea seems to be supported by the average focal length of our vehicle-treated lenses (14.1±0.2 mm; data not shown), which was shorter and therefore more powerful than the vehicle-treated lenses in Luck and Choh's study (19.6 mm). It is possible that in our experiment, lenses were maximally rounded and therefore, any further release of tension associated with the actin-myosin network would be too small to detect.

Indications that cytoskeletal proteins might play a role in lenticular biomechanics were noted by Rafferty et al. [39], who showed that increasing intracellular calcium levels in rabbit anterior epithelial cells in the lens resulted in changes in actin stress fiber distributions. Although the concentration of myosin is generally lower than actin in contractile networks, such as those found in lens epithelial cells [14], it is nonetheless crucial for structural integrity. Two of the disruptors used targeted myosin or myosin function and both were able to exert effects that were similar to those exerted by the actin disruptor. However, it should also be noted that cytoskeletal integrity is not limited to the actomyosin system; intermediate filaments and microtubules also play a role in maintaining the cellular architecture [8]. Lenses from mice

in which a gene for beaded filaments, which belongs to the intermediate filament gene family, is knocked out are less stiff than those from wild-type mice are [17]. Our results add to the growing body of evidence showing the importance of cytoskeletal protein integrity to lenticular biomechanics. While studies by Fudge et al. [17] and the present study examined how disrupting cytoskeletal integrity affects the biomechanics of the lens as a whole, a previous study investigated their effects on lenticular cells individually. Unlike our results, Hozic et al. [40] showed no difference in the stiffness of the individual lenticular cells with cytochalasin, an actin disruptor. The difference between the present study and that of Hozic et al. [40] may be related to the disruptor used (latrunculin versus cytochalasin B); cytochalasin works by inhibiting actin polymerization, essentially preventing the formation of actin networks (blocks monomer addition), while latrunculin depolymerizes f-actin.

In both the acute and longitudinal compression trials, lenses were kept in TS in temperatures at or above 5 °C to retard cell metabolism and prevent the tissue from degrading, particularly for the longitudinal trials that required ex vivo viability for durations greater than 32 h. It should be noted that lenses in situ would be closer to body temperature [41]; moreover, cold temperatures could promote the depolymerization of actin microfilaments. Hall et al. [42,43] showed that cells exposed to a temperature of 4 °C for 2–4 h exhibit a marked thinning of actin filaments. However, Matthews et al. [44] found no effects of these conditions on the actin structure. Our lenses were exposed to a minimum of 5 °C for a maximum of 15 min, and thus the cold-induced depolymerization of f-actin should have been minimal. Furthermore, any cold-induced depolymerization was accounted for by our control lenses, which experienced identical conditions aside from the disruptor treatment.

The confocal imaging and western blots together indicate that the disruptors penetrated the lens at a deep enough level to affect the cytoskeletal distribution at the BMC in addition to the lens fiber cells. Given that confocal images were acquired between 12 and 13 µm below the lens capsule, it is known that the depth of the disruptor penetration is at least to this extent. It is unclear how deeply the disruptors penetrate the lens, as well as whether they diffuse uniformly throughout the lens; however, it is sure to be different, as a disparity between the diffusion patterns at the surface of the lens compared to the lens core syncytium exists and has been shown by Shestapolov and Bassnett [45,46].

While f-actin depolymerization was an expected outcome of latrunculin treatment, myosin organization was also affected (Figure 6A). It has been proposed that in order

for myosin II to remain in the cytoskeleton, it must be bound to stable actin [47]. Similarly, blebbistatin also appears to enhance the depolymerization of f-actin (Figure 6C). Blebbistatin is known to disassemble actin [48], presumably by reducing myosin activity and therefore actin cross-linkings. Although ML-7 affects phosphorylation and therefore the ability of actin and myosin to interact, it would not be expected to physically alter the architecture of the actomyosin network, which was indeed the case (ML-7-treated R_n = 2.02±0.02 versus vehicle-treated R_n = 2.01±0.02; data not shown).

Our results showed that despite the cytoskeletal distribution changes at the BMC and the measured changes in stiffness, the optics of the isolated lenses were unaffected by the disruptors (Table 1), and during the acute study trials, it was noted that lenses maintained transparency (note the clarity of the lens in Figure 1). Either the disruption at the BMC was too small to confer a change in SA and scatter, or the regular arrangement and tight packing of the lens fiber cells rendered any disruption of the actomyosin distributions negligible. However, while lenses were clear during the acute experiment, the long-term effects of disruptors on lenticular transparency remain unknown; a qualitative assessment of the lenses indicated that incubation with disruptors for about 1 h resulted in turbidity and the development of cataracts (data not shown). Whether turbid lenses can recover optical clarity also remains unknown; therefore, the use of cytoskeletal disruptors as permanent effectors for changing lens biomechanics must take into account other possible effects on functions such as optical clarity.

Other questions that need to be answered include whether these disruptors can be as effective on older lenses. As mentioned above, the focus of this experiment was to determine whether disruption of the actomyosin lattice could alter lenticular biomechanics, and for experimental convenience, we used young chicks. While it is tempting to relate our results to presbyopia, which is accompanied by profound increases in lenticular stiffness with age [49-51], further investigations will require the use of older experimental animals.

We have found that by targeting the cytoskeletal proteins that are known to have structural roles in cells, lenses become less stiff, but whether the lens plays more than a passive role during accommodation remains unclear. The physiology and cellular arrangement of the lens are mostly dedicated to maintaining optical clarity by ordering the fiber cells into a regular arrangement and reducing the intercellular spaces between them so light is less scattered. The hexagonal shape conferred upon the lens fiber cells fulfils both functions and therefore,

the finding that a geodesic hexagonal network is present at the posterior surface may simply reflect the shape of the highly organized fiber cells and function to resist deformations that could disrupt this organization.

In summary, we found that the disruption of actomyosin networks in young avian lenses causes significant decreases in the stiffness of isolated lenses, but there are no differences in their optical properties. These results are consistent with the hypothesis that lens stiffness may be actively tuned via adjustments to the actomyosin networks in lens cells. The lack of an effect on lens optical properties may have been due to a "rounding up" artifact caused by the isolation of the lens from the eye.

ACKNOWLEDGMENTS

REFERENCES

1. Helmholtz Hv. Helmholtz's treatise on physiological optics. Translated from the 3d German ed. Southall JPC, editor. New York: Dover Publications; 1962. 3 v. in 2. illus. (part col.) p.

2. Sivak JG. Accommodation in vertebrates: a contemporary survey. Curr Top Eye Res 1980; 3:281-330. [PMID: 7344838].

3. Zinn JG, Wrisberg HA. Iohannis Gottfried Zinn ... Descriptio anatomica oculi humani iconibus illustrata. Nunc altera vice edita, et necessario supplemento, nouisqve tabvuis aucta ab Henr. Aug. Wrisberg. ed. Goettingae: Apud viduam B. Abrami Vandenhoeck 1780; 248:7-.

4. Bettelheim FA. Physical Basis of Lens Transparency in the Ocular Lens: Structure, Function, and Pathology. New York: Marcel Dekker Inc.; 1985.

5. Clark JI, Matsushima H, David LL, Clark JM. Lens cytoskeleton and transparency: a model. Eye (Lond) 1999; 13:Pt 3b417-24. [PMID: 10627819].

6. Maddala R, Deng PF, Costello JM, Wawrousek EF, Zigler JS, Rao VP. Impaired cytoskeletal organization and membrane integrity in lens fibers of a Rho GTPase functional knockout transgenic mouse. Lab Invest 2004; 84:679-92. [PMID: 15094715].

7. Ireland M, Lieska N, Maisel H. Lens actin: purification and localization. Exp Eye Res 1983; 37:393-408. [PMID: 6357816].

8. Quinlan RA, Sandilands A, Procter JE, Prescott AR, Hutcheson AM, Dahm R, Gribbon C, Wallace P. The eye lens cytoskeleton. Eye (Lond) 1999; 13:Pt 3b409-16. [PMID: 10627818].

9. Alberts B. Molecular biology of the cell. 5th ed. New York: Garland Science; 2008.

10. Rao PV, Maddala R. The role of the lens actin cytoskeleton in fiber cell elongation and differentiation. Semin Cell Dev Biol 2006; 17:698-711. [PMID: 17145190].

11. Kamm KE, Stull JT. The function of myosin and myosin light chain kinase phosphorylation in smooth muscle. Annu Rev Pharmacol Toxicol 1985; 25:593-620. [PMID: 2988424].

12. Hai CM, Murphy RA. Cross-bridge phosphorylation and regulation of latch state in smooth muscle. Am J Physiol 1988; 254:C99-106. [PMID: 3337223].

13. Yuen SL, Ogut O, Brozovich FV. Nonmuscle myosin is regulated during smooth muscle contraction. Am J Physiol Heart Circ Physiol 2009; 297:H191-9. [PMID: 19429828].

14. Rafferty NS, Scholz DL, Goldberg M, Lewyckyj M. Immunocytochemical evidence for an actin-myosin system in lens epithelial cells. Exp Eye Res 1990; 51:591-600. [PMID: 2249732].

15. Bassnett S, Missey H, Vucemilo I. Molecular architecture of the lens fiber cell basal membrane complex. J Cell Sci 1999; 112:2155-65. [PMID: 10362545].

16. Yeh S. W. Liou, N. S. Rafferty. Polygonal Arrays of Actin Filaments in Human Lens Epithelial Cells. Invest Ophthalmol Vis Sci 1986; 27:1535-1540. [PMID: 3759370].

17. Fudge DS, McCuaig JV, Van Stralen S, Hess JF, Wang H, Mathias RT, FitzGerald PG. Intermediate filaments regulate tissue size and stiffness in the murine lens. Invest Ophthalmol Vis Sci 2011; 52:3860-7. [PMID: 21345981].

18. Ramaekers FC, Poels LG, Jap PH, Bloemendal H. Simultaneous demonstration of microfilaments and intermediate-sized filaments in the lens by double immunofluorescence. Exp Eye Res 1982; 35:363-9. [PMID: 6754403].

19. Kibbelaar MA, Ramaekers FC, Ringens PJ, Selten-Versteegen AM, Poels LG, Jap PH, van Rossum AL, Feltkamp TE, Bloemendal H. Is actin in eye lens a possible factor in visual accomodation? Nature 1980; 285:506-8. [PMID: 6995847].

20. Kuszak JR, Zoltoski RK, Tiedemann CE. Development of lens sutures. Int J Dev Biol 2004; 48:889-902. [PMID: 15558480].

21. Luck S, Choh V. Effects of a myosin light chain kinase inhibitor on the optics and accommodation of the avian crystalline lens. Mol Vis 2011; 17:2759-64. [PMID: 22065929].

22. Choh V, Sivak JG, Meriney SD. A physiological model to measure effects of age on lenticular accommodation and spherical aberration in chickens. Invest Ophthalmol Vis Sci 2002; 43:92-8. [PMID: 11773018].

23. Morton WM, Ayscough KR, McLaughlin PJ. Latrunculin alters the actin-monomer subunit interface to prevent polymerization. Nat Cell Biol 2000; 2:376-[PMID: 10854330].

24. Spector I, Shochet Y, Kashman A. Latrunculins: novel marine toxins that disrupt microfilament organization in cultured cells. Science 1983; 219:493-5. [PMID: 6681676].

25. Kovács M, Toth J, Hetenyi C. Malnasi-Csizmadia, A., Sellers, J. R. Mechanism of Blebbistatin Inhibition of Myosin II. J Biol Chem 2004; 279:35557-63. [PMID: 15205456].

26. Saponara S, Fabio F, Sgaragli G, Maurizio C, Hopkins B, Bova S. Effects of commonly used protein kinase inhibitors on vascular contraction and L-type calcium current. Biochem Pharmacol 2012; 84:1055-1061. [PMID: 22884855].

27. Demer LL, Yin FC. Passive biaxial mechanical properties of isolated canine myocardium. J Physiol 1983; 339:615-30. [PMID: 6887039].

28. Higashita R, Sugawara M, Kondoh Y, Kawai Y, Mitsui K, Ohki S, Tange S, Ichikawa S, Suma K. Changes in diastolic regional stiffness of the left ventricle before and after coronary artery bypass grafting. Heart Vessels 1996; 11:145-51. [PMID: 8897063].

29. Weeber HA, van der Heijde RG. Internal deformation of the human crystalline lens during accommodation. Acta Ophthalmol 2008; 86:642-7. [PMID: 18752516].

30. Sivak JG, Ryall LA, Weerheim J, Campbell MC. Optical constancy of the chick lens during pre- and post-hatching ocular development. Invest Ophthalmol Vis Sci 1989; 30:967-74. [PMID: 2722451].

31. Sivak JG, Kreuzer RO. Spherical aberration of the crystalline lens. Vision Res 1983; 23:59-70. [PMID: 6603055].

32. Glasser A, Howland HC. In vitro changes in back vertex distance of chick and pigeon lenses: species differences and the effects of aging. Vision Res 1995; 35:1813-24. [PMID: 7660588].

33. Irving EL, Sivak JG, Curry TA, Callender MG. Chick eye optics: zero to fourteen days. J Comp Physiol 1996; 179:185-94. [PMID: 8765557].

34. Pollard TD. Rate constants for the reactions of ATP- and ADP-actin with the ends of actin filaments. J Cell Biol 1986; 103:2747-54. [PMID: 3793756].

35. Sinard JH, Pollard TD. Acanthamoeba myosin-II minifilaments assemble on a millisecond time scale with rate constants greater than those expected for a diffusion limited reaction. J Biol Chem 1990; 265:3654-60. [PMID: 2303471].

36. Kuhn JR, Pollard TD. Real-time measurements of actin filament polymerization by total internal reflection fluorescence microscopy. Biophys J 2005; 88:1387-402. [PMID: 15556992].

37. Takizawa N, Ikebe R, Ikebe M, Luna EJ. Supervillin slows cell spreading by facilitating myosin II activation at the cell periphery. J Cell Sci 2007; 120:3792-803. [PMID: 17925381].

38. Glasser A, Murphy CJ, Troilo D, Howland HC. The mechanism of lenticular accommodation in chicks. Vision Res 1995; 35:1525-40. [PMID: 7667911].

39. Rafferty NS, Rafferty KA, Ito E. Agonist-induced rise in intracellular calcium of lens epithelial cells: effects on the actin cytoskeleton. Exp Eye Res 1994; 59:191-201. [PMID: 7835408].

40. Hozic A, Rico F, Colom A, Buzhynskyy N, Scheuring S. Nano-mechanical characterization of the stiffness of eye lens cells: a pilot study. Invest Ophthalmol Vis Sci 2012; 53:2151-6. [PMID: 22427595].

41. Al-Ghadyan AA, Cotlier E. Rise in lens temperature on exposure to sunlight or high ambient temperature. Br J Ophthalmol 1986; 70:421-6. [PMID: 3718905].

42. Hall SM, Haworth SG. Effect of cold preservation on pulmonary arterial smooth muscle cells. Am J Physiol 1996; 270:L435-45. [PMID: 8638736].

43. Hall SM, Komai H, Reader J, Haworth SG. Donor lung preservation: effect of cold preservation fluids on cultured pulmonary endothelial cells. Am J Physiol 1994; 267:L508-17. [PMID: 7977761].

44. Matthews JN, Yim PB, Jacobs DT, Forbes JG, Peters ND, Greer SC. The polymerization of actin: extent of polymerization under pressure, volume change of polymerization, and relaxation after temperature jumps. J Chem Phys 2005; 123:074904-[PMID: 16229617].

45. Shestopalov VI, Bassnett S. Development of a macromolecular diffusion pathway in the lens. J Cell Sci 2003; 116:4191-9. [PMID: 12953070].

46. Shestopalov VI, Bassnett S. Expression of autofluorescent proteins reveals a novel protein permeable pathway between cells in the lens core. J Cell Sci 2000; 113:1913-21. [PMID: 10806102].

47. Kolega J, Kumar S. Regulatory light chain phosphorylation and the assembly of myosin II into the cytoskeleton of micro-capillary endothelial cells. Cell Motil Cytoskeleton 1999; 43:255-68. [PMID: 10401581].

48. Martens JC, Radmacher M. Softening of the actin cytoskeleton by inhibition of myosin II. Pflugers Arch 2008; 456:95-100. [PMID: 18231808].

49. Helmholtz H. Über die Akkommodation des Auges. Albrecht v Graefes Arch Ophthalmol 1855, 1: 1–74. 1855;1;1–74.

50. Gilmartin B. The aetiology of presbyopia: a summary of the role of lenticular and extralenticular structures. Ophthalmic Physiol Opt 1995; 15:431-7. [PMID: 8524570].

51. Brown N. The change in shape and internal form of the lens of the eye on accommodation. Exp Eye Res 1973; 15:441-59. [PMID: 4702379].